ScicncePG
Science Publishing Group

Research on Flow Characteristics of Upstream Cavity with Labyrinth Seals in Axial Compressor

Xin Fu[*], Yingying Xu, Yan Zhang

College of Energy and Power Engineering, Nanjing University of Aeronautics and Astronautics, Nanjing, China

Email address:

fu_xin@nuaa.edu.cn (Xin Fu), xuyingy18@163.com (Yingying Xu), 2224627591@qq.com (Yan Zhang)

[*]Corresponding author

Abstract: The sealing between rotating components and stator components has become one of the main issues to be studied in the compressor. The mixing of stator root leakage flow and the mainstream can seriously affect the performance of the compressor. This article does a series of work on numerical calculation of plane diffuser cascade with the stator cavity and three-stage labyrinth seal. It also analyzes the details of the flow structure on upstream cavity. In this paper, the 3D streamlines distribution of the cascade corner region is studied, respectively for the no leakage case and the mixing mechanism of the secondary flow and mainstream with leakage. On this basis, the upstream cavity configuration is optimized and some results are obtained as fellows. The mainstream in the blade leading edge into the upstream cavity comes into being the secondary flow, which similar to leakage flow. It can affect the highest 80% leaves of the high range. Leakage flow is mainly influence on the performance of the blade root flow field and weakly of next to casing area. Compared to no leakage case, angular separation position ahead of time and range increased when there is leakage. Thus, added rib on both sides of the vessel wall can reduce the total pressure loss of the S3 section, and the relative position of ribbed effect significantly. The research shows that first layer of rib is better when set on the hub wall surface, the total pressure loss coefficient decreased by 3.49%.

Keywords: Aerospace Propulsion Theory and Engineering, Blade Root Leakage, Sealing Labyrinth Seals, Upstream Cavity, Secondary Flow

1. Introduction

Clearance leakage flow is one of the mainstream characteristics in aero engine compressor, and stator root leakage plays a significant role in this process. There are two different structures of compressor stator blades, and both of them have different influences on the engine [1, 2]. However, neither of them can completely inhibit the formation of leakage flow, and sealing has become one of the key problems in compressor research [3]. In order to reduce leakage and improve efficiency, various sealing measures are usually needed to maintain the working pressure between each chamber, especially the pressure of rotor and stator. The labyrinth seal is a kind of widely used non-contact seal structure with simple structure, reliable performance and long service life. As the aircraft engine technology matured, it is very difficult to further improve the performance of impeller machine by improving aerodynamic design and other basic means. Relatively, to improve and develop new seal technology and improve the engine performance compared with other parts, is a kind of effective and less cost way. Improvement of sealing technology can greatly improve the performance of future aircraft engines [4].

Wellborn studied the blade root leakage flow and its effect on the compressor performance, results show that about 0.5% of the leakage can be caused the rotor efficiency and total pressure loss of about 1.5% and 1% respectively [5-7]. Heidegger researched the flow of parameterized numerical simulation in a high speed compressor chamber, the main conclusions are as follows, leakage flow through the upstream cavity tangential velocity increased from 0 to 75% of the wheel linear velocity, the leakage flow in the process of total temperature rose sharply. Import and export of vortex

chamber should drag power is not caused by adjacent rotor suction effect, and mainly from the mainstream and the effect of leakage flow. The analysis of the radial flow parameters shows that the stator flow near the hub has an effect on the flow at the inlet and outlet of the blade root and cavity in the range of -10%~0 blade height. The tangential velocity and total temperature increase rapidly in this region that the flow parameters in other regions of the cavity are more uniform [8]. Popovic changed the upstream cavity of a high-pressure turbine stator into an overlapping seal structure to simulate the influence on the leakage flow, and the results show that vessel geometry size smaller change can cause mainstream pressure loss bigger fluctuation [9]. Demargne first pointed out with the increase of the tangential velocity, the blade angle area separation was effectively suppressed. Research also pointed that the influence caused by tangential velocity affects the entire channel span flow angle and the distribution of the loss [10].

Through the experiment and calculation research, Kim found that due to high-loss flow into the downstream cavity, the loss of stator vane channels decreased in the downstream. Additionally, the leakage flow tangential speed increase will weaken the suction side of the shedding vortex [11, 12].

Xin. F took the plane diffuser cascade as the research object, studied the flow conditions in the upstream cavity in detail and analyzed the total pressure loss caused by the leakage flow. Studies show that when the clearance blade height ratio changes from 1.0% to 0.5%, the leakage flow decreases by 53% and the total pressure loss coefficient decreases by 1.784%, the secondary flows in the upstream cavity increases. Therefore, in order to reduce the influence of secondary flows in the blade root on the mainstream, the flow condition of secondary flows in the upstream cavity must be considered [13].

Yong-hua Cao against a real size direct amplification of type seal tooth model for two-dimensional experimental study of reverse jet, at the same time made a series of numerical simulation research. The study found that the size of the reverse jet position decision of inverse vortexes size and the deflection direction of leakage flow in the second tooth, and the angle of jet flow determines the slowing down effect on the axial velocity of leakage flow. As 45° and at middle of first tooth cavity of the jet position, the leakage coefficient decreases by 11.5% compared with that without jet [14].

From previous studies, researchers mostly deal with the leakage flow of the stator blade root directly by setting the gap with the hub, and the focus is mainly on the complex vortex structure and less on the influence of the real stator structure. Actually, for belted stator, leakage flow interacts with the labyrinth gas seal cavity and upstream and downstream cavity flow, which influenced the leakage flow cannot be ignored.

2. Calculation Model and Method

2.1. Calculation Model

The geometry modeling of actual sealing structure is complicated, thus, researchers often retain significant flow and structural characteristics in numerical calculation, while simplifying other parts. This paper references simplified model used in the study of Kim's [12], which consists with three labyrinths, platforms, bushings, wheels, and the diffusion blade. The leaf type reference a stator blade root section of a compressor provided by China Gas Turbine Research Institute and specific parameters is shown in Table 1 [15].

Compared with the simple configuration of trapezoidal single tooth in Kim's model, the configuration used in this paper is relatively complex, and has been verified by a large number of experiments by the research group. The labyrinth modeling parameters are shown in Figure 1, for the leakage clearance is 0.7mm, the thickness of the top of the labyrinth is 0.2mm, the width of the labyrinth cavity is 4mm, and the depth of the cavity is 4.3mm. The top of the blade is connected with the fixed casing, and the bottom of the blade junction of the hub is connected with the bushing. The computational domain has a total chord length of 4 times along the flow direction, including 1 times for the inlet chord length and 2 times for the exit chord length, and the computational domain length along the frontal line is a grid spacing.
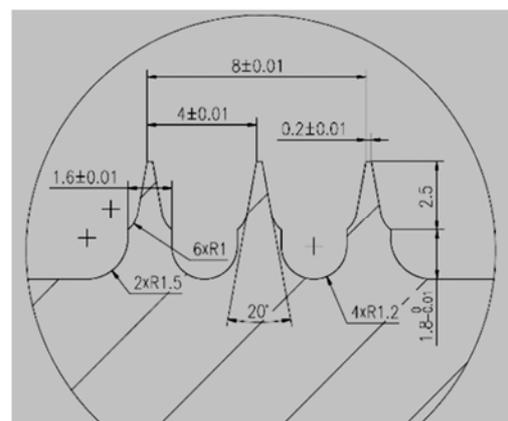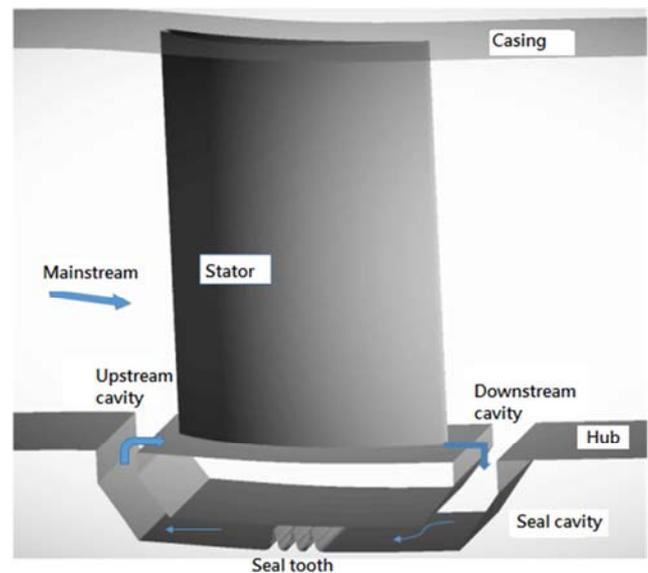

*Figure 1. Calculation model and structure parameter.*

Table 1. *Model size parameter.*

Nomenclature	Value	Nomenclature	Value
C / mm	60	C_z / mm	56.2
S / mm	45	H / mm	80
τ	1.33	E / mm	0.7
k_1 / °	46	k_2 / °	-10
h / mm	5	D / mm	9

## 2.2. Computational Grid and Boundary Conditions

ANSYS ICEM CFD software is used in this paper. As shown in Figure 2, the computational domain is divided into 14 blocks of cascade channel and 67 blocks of seal cavity. In order to improve the grid orthogonality of the cascade surface, O-type grid is adopted around the blade, H-type grid for the remaining part, y+ number control within 2 near wall.

The study found that, when entrance Mach number is 0.1, inlet flow angle is 9°, the influence of leakage flow on the mainstream is most obvious and exit total pressure loss is most serious. Thus, boundary conditions are as follows: setting the total import temperature as 288.15K, total pressure as 101325pa, setting the blade row along the circumferential as periodic boundary, at the same time, the solid wall been set to the adiabatic, no slip boundary condition, and the under wall velocity given to 32m/s.
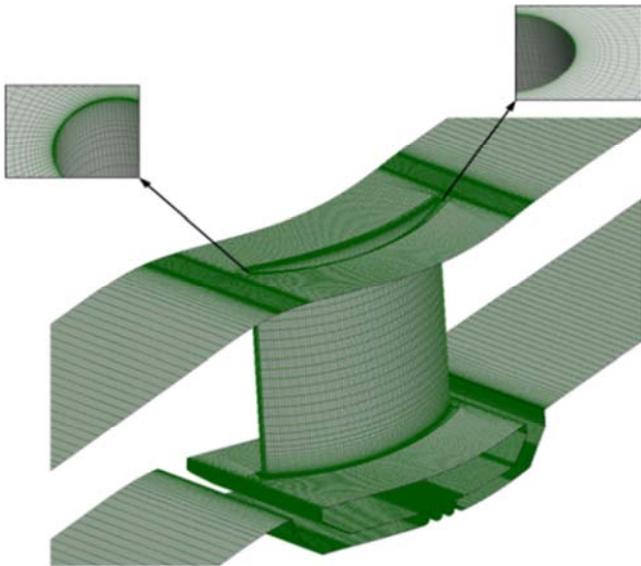
**Figure 2.** *Schematic diagram of computational grid.*

2.3. Calculation Accuracy Verification

It is necessary to verify the accuracy of the calculation model and compare the aerodynamic loss caused by the sealing structure. Thus, paper calculated the static pressure distribution on the pressure surface and suction surface under the condition of no sealing clearance, and compared with the experimental results in literature 14. The results show that the calculated results were in good agreement with the experimental results as shown in Figure 3. BSL k-ω model was selected as the calculation model.
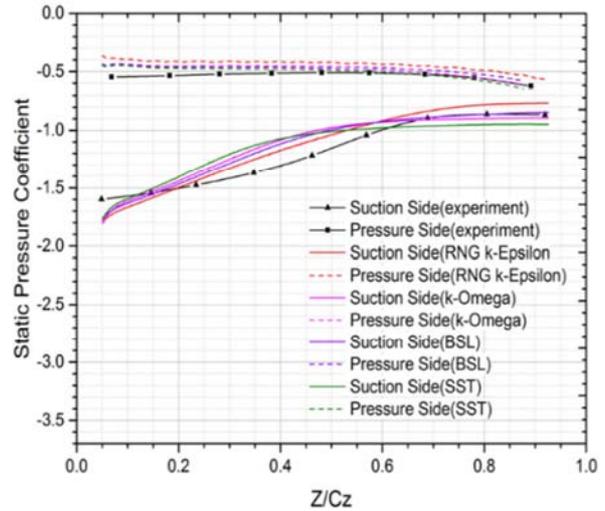
Figure 3. *Experimental and simulated static pressure distribution.*

2.4. Grid Independence Verification

The calculation result will be distorted for the number of meshes is too small, and if the number of meshes is too large, the calculation amount will be increased, and the computing resources will be excessively occupied. So in this paper, on the premise of guaranteeing the quality of the grid, six groups of grids are selected for independent verification. For each group of grids, the same turbulence model and boundary conditions, as well as the same Mach number and inlet flow angle were used. As shown in Figure 4, when the number of grids was about 3.5 million, the flow in the channel remains around 9.402×10^{-2}kg/s, and the flow basically remains unchanged when the number of grids was increased in the future. Therefore, the number of subsequent computational grids was set at about 3.5 million.
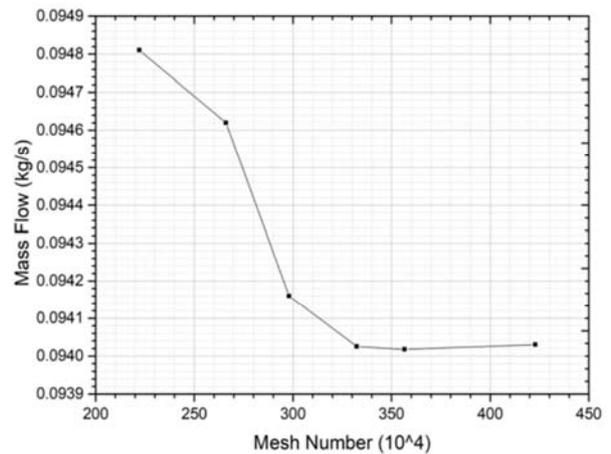
Figure 4. *Grid Independence Verification.*

3. Secondary Flow Structure and Effect of Performance

3.1. Flow Field Structure of Secondary Flow

In this section, it analyzed the flow structure of the root of

the cascade and the secondary flow structure in the upstream cavity. Since the blade row is provided with a periodic boundary along the circumferential direction, the disconnection of the flow line indicates the flow into the adjacent period channel or from the adjacent period channel, and expresses in the same period. In order to know the total pressure loss of the fluid after passing through the cascade passage, the loss coefficient is defined as follows:

$$\text{Yp} = \frac{p_{in}^* - p^*}{p_{in}^* - p_{in}} \qquad (1)$$

Where p_{in}, p_{in}^* are the inlet static pressure and total pressure, and p^* is the total pressure of 130% axial chord section.

As shows in Figure 5, the blue streamline indicates the secondary flow structure generated by the mainstream entering the upstream cavity, and the cyan streamline indicates leakage flow. These two flow structures constitute a complex secondary flow in the upstream cavity.

From Figure 5, the blue fluid starts from the leading edge region of the blade. In the upstream cavity, a portion of the blue forms a clockwise vortex and then flows with the leakage flow to the middle of the cascade channel; another portion of the fluid flows down the wall. Finally, under the action of the leakage flow, the direction is changed. The blue fluid climbs up the wall and flows out of the upstream cavity. These two parts flow mixed with mainstream in the cascade channel. Then, at the exit of the blade, it is divided into two parts again: for one flows out with the channel vortex, for another climb in the direction of leaf height, which can affect the flow in the 80% leaf height range together with the leakage flow.

The study found that the secondary flow of the upstream cavity is more obvious at the leading edge of the cascade but has no obvious performance in other areas. The preliminary analysis shows the radial velocity of the leakage flow cancels the radial velocity of the mainstream, and the mainstream of the channel is slightly upward which does not develop into the secondary flow. At the leading edge of the blade, due to the deflection to suction surface of the leakage flow here, the ability to reduce the mainstream radial velocity is weakened. The secondary flow finally flows into the cascade channel together with the leakage flow.

It can be seen from Figure 6 that the flow structure of the cyan streamline in the upstream cavity is more complicated due to the presence of the blue flow. The cyan mainly comes from the airflow near the end wall of the pressure surface. The static pressure increases after passing through the diffuser cascade channel, so that the pressure at the downstream cavity is significantly higher than that of the upstream cavity. Driven by the differential pressure, the fluid near the end wall enters the downstream cavity. The fluid velocity initially entering the cavity is higher, and the fluid flows downward against the wall. During this process, the fluid kinetic energy is gradually attenuated, eventually forming a wide range of vortices in the downstream cavity.
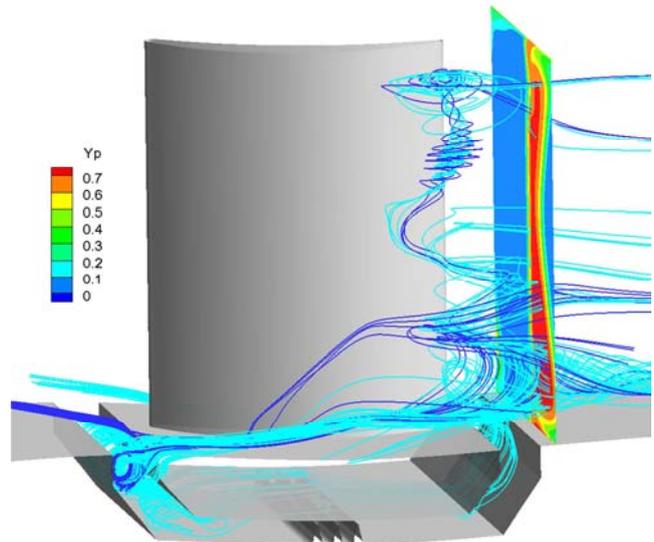

*Figure 5.* Cascade passage secondary flow structure.
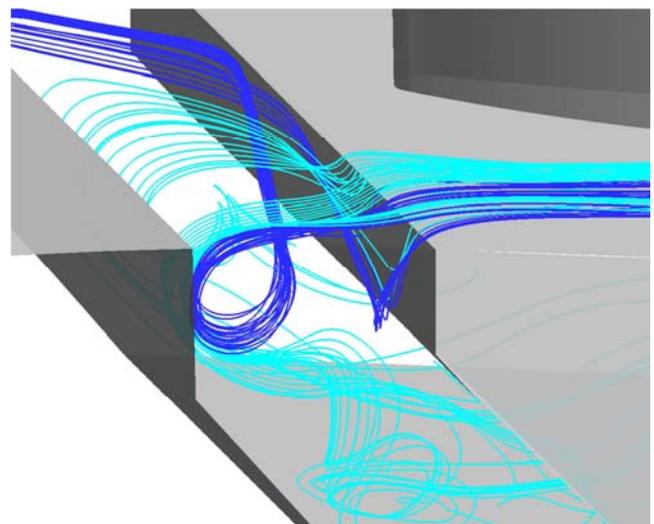
Figure 6. Upstream cavity secondary flow structure.
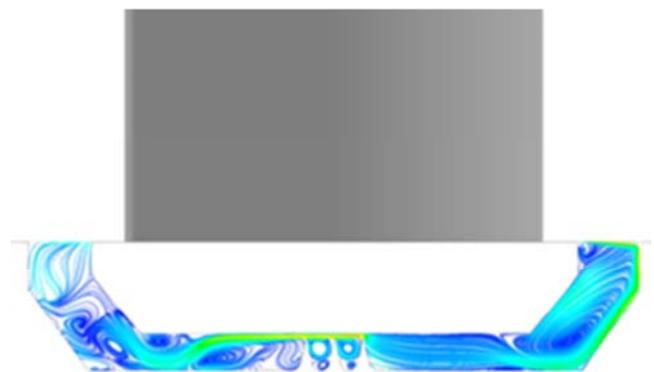
Figure 7. Section streamline of channel.

Due to the small space and the weakening of fluid kinetic energy after passing through the downstream cavity, a plurality of distinct dissipative vortices can be seen in the seal cavity and the upstream cavity (as shown in Figure 7), causing a large amount of low-energy fluid to accumulate in the

upstream cavity. Under the action of the higher-speed mainstream, part of the fluid moves downstream with the mainstream, finally circulated by the channel vortex at the outlet. The other part flows to the suction angle under the action of the lateral pressure gradient, and climbs along height of the leaf blended with the low-energy fluid, which can affect the range of 80% leaf height.

3.2. Influence of Secondary Flow on Flow Structure of Cascade Passage

In this section, the gapless cascade (no leakage flow and secondary flow) is used as a comparison to analyze the influence of the secondary flow on the flow structure and performance of the cascade channel.

Firstly, the flow field structure of the gapless cascade channel is analyzed. It can be seen from Figure 8 that the blue fluid moves toward the wall surface under the lateral pressure gradient and is divided into two branches at the near wall surface. One climbs up at the vicinity of the suction surface under the action of the end wall boundary layer, then, produces local reflux for mixing with trailing edge airflow in the range of about 30% to 35% blade height. While the other branch flows along the blade root, separation occurs at 130% axial chord length and 10% blade height near the trailing edge. The light blue fluid rises in the direction of the blade height and separates on the surface of the blade. One part of the fluid generates a large recirculation zone due to the lower initial kinetic energy, the other part flows directly downstream of the recirculation zone. The purple fluid flows to the suction face after separated at the leading edge of the blade, and mix with the blue fluid at about 80% of axial chord length. Observing the flow field details of the blade trailing edge, it can be found that the secondary flow accumulation in the blade root zone is the most serious, where also the main source of total pressure loss.

Combining with the above analysis, the fluid separation mainly starts at the proximal wall boundary layer. Under the lateral pressure gradient, the low-energy fluid on the pressure surface side is continuously accumulated on the suction side, which causes the main direction to deflect. Due to the phenomenon that the flow from the pressure side to the suction side of the blade trailing edge, the complexity of corner flow is further increased. Therefore, the three-dimensionality of the flow from the corner to the trailing edge exit section is greatly increased, resulting in a sharp drop in the flow performance of the cascade.

Figure 9 shows streamline of the cascade passage with leakage. It can be seen from the figure that the secondary flow structure of the cascade passage is more complex and has a wider influence on the mainstream when there is the blade root leakage. Firstly, the white fluid flowing near the suction surface along the leading edge of the blade was rapidly lifted and separated at the 27% of axial chord length. Due to the effect by the leakage flow, the light blue streamline starts from the leading edge of the blade rather than the middle area of the blade.

At the same time, the fluid kinetic energy is improved

driven by the leakage flow, and no large-scale reflux area is generated in the corner area. The blue fluid also starts at the leading edge of the blade. Relatively no leakage, this part of fluid is divided into two branches at the advantage of 60% axial chord. One branch fluid mixing with the white fluid, rises along the blade surface after a small range of backflow. The other branch fluid separates again for one involved in the large-scale channel vortex at the trailing edge, while the other fluid inhaled into leakage flow. Pink streamline is the development of the upstream boundary layer fluid in the cascade channel. The fluid is affected by the channel vortex after 60% axial chord length. And the flow range is significantly increased, separated at 130% axial chord length: a part moves downstream with the channel vortex, the other part fluid climbs toward the height of the blade and finally forms a concentrated shedding vortex in the range of 30% to 50% height.
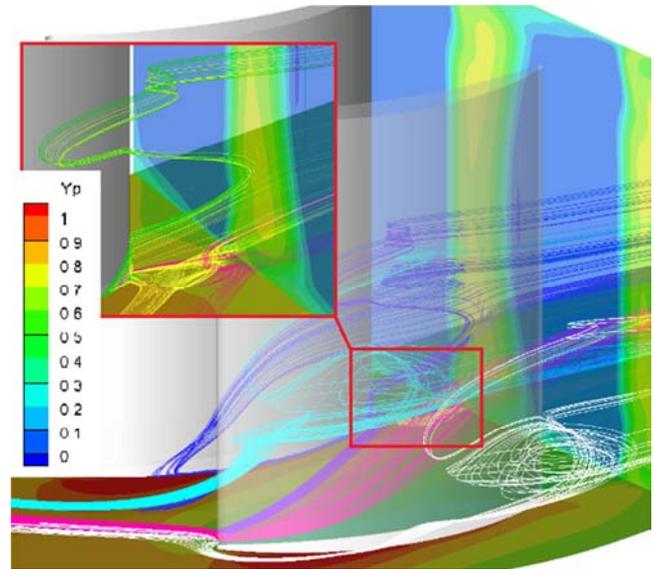

**Figure 8.** *Flow field structure of no clearance cascade channel.*
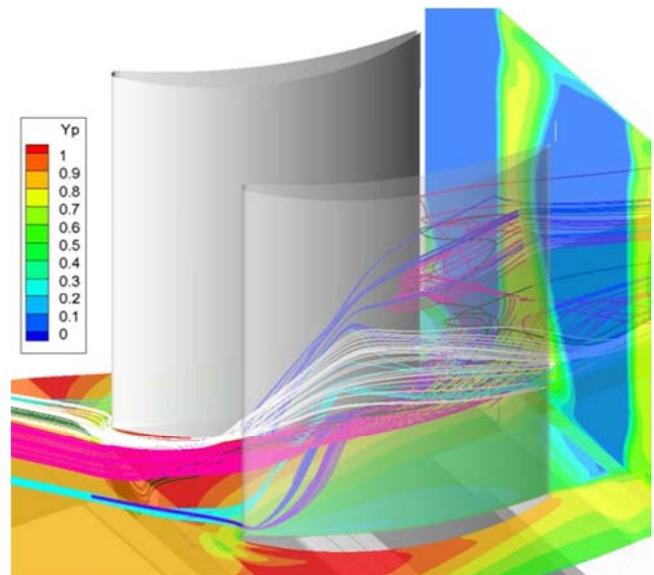
Figure 9. *Flow field structure of gap cascade channel.*

3.3. Influence of Secondary Flow on Performance of Cascade Passage

In order to know the influence of the secondary flow in the upstream cavity, a model with a tip clearance of 0.4 mm is added as a comparison (other parameters are unchanged). The gap cascade channel loss is divided into the upstream cavity secondary flow loss, leakage flow loss and other losses (approximated loss of gapless cascade, quantified as gapless total cascade loss coefficient: Yp = 0.2283). Here, the flow percentage is used instead of the loss to quantify the secondary flow loss in the upstream cavity. The analysis results are shown in Table 2.

It can be seen from Table 2 that the rate of secondary flow is greater than the rate of leakage flow. When seal-clearance is exist, the smaller the clearance, the smaller the flow rate of the leakage flow, the larger the flow rate of the secondary flow and is much larger than the leakage flow. At the same time, due that the leakage gap decreased from 0.7mm to 0.4mm, the total pressure loss coefficient decreased by 2.3%. Among that, the loss caused by the leakage flow is reduced by 19.4% compared with the change of the gap, but the loss caused by the secondary flow is increased by 4.6%. It can be seen that the leakage flow and the secondary flow are in a trade-off relationship. Simply reducing the leakage gap does not completely reduce the total pressure loss.

Table 2. *Secondary flow loss coefficient.*

Leakage gap	Leakage flow / Mainstream (%)	Secondary flow / Mainstream (%)	Yp (130% axial chord length)	Yp (secondary flow loss)	Yp (Leakage flow loss)
0mm	0	0	0.2283	0	0
0.4mm	0. 2887	0. 7132	0. 2486	0. 0113	0. 0116
0.7mm	0. 4714	0. 4829	0. 2545	0. 0108	0. 0144

Figure 10 shows the distribution of the total pressure loss coefficient in three cases along the height of the blade about the 130% section in the circumferential direction. The total pressure loss of middle blade is the smallest when there is no leakage, and the loss increases symmetrically on both sides of the end wall. When there is leakage, the gap change only changed the total pressure loss coefficient. Under the two gap conditions, the regularities of distribution are basically the same: the total pressure loss in the boundary layer does not change much. And at the 10% section of height, the pressure loss is the largest, corresponding channel vortex core position. At the position above 42% of the height, due to the "pumping" effect in the low pressure zone of the downstream cavity, some of the low-energy fluid moves downward, which slows down the accumulation of the secondary flow in the corner zone. Thus the loss coefficient decreases when there is leakage. Overall, the loss of the interface increases with leakage, and the loss of root zone is still the main source.


Figure 10. *Distribution of total pressure loss at 130%.*

4. Configuration Studies of Upstream Cavity

Based on the foregoing, it can be found that the existence of the gap makes the total pressure loss of the cascade significantly increased. Although the sealing gap can reduce the total pressure loss effectively, the sealing gap cannot be reduced indefinitely. In this case, it must be started from other aspects to reduce losses. The secondary flow can affect the flow in a range of 80% height, which cannot be neglected. Compared with changing the structure of the caries and the sealing gap, it is much simpler to optimize from the secondary flow of the upstream cavity.

In order to prevent the secondary flow entering to upstream cavity, a center-symmetrical two-row rib structure is disposed at both side walls of the upstream cavity. As shown in Figure 11, the rib width is set to 3/4 cavity width, and the height is set to 1/5 cavity height, the relative positions of Case 1 and Case 2 ribs are different, and the tip clearance is 0.7mm.

Figure 12 shows the total pressure loss coefficient nephograms at 130% of the axial chord length under three operating conditions. The results show that the ratio of secondary flow to mainstream flow is 0.24% and 0.30% respectively in case 1 and 2.

Figure 13 is the flow situation of leakage flow in the cascade passage and the cloud diagram of total pressure loss of S3 section in the three cases. The positions of S3section are 25%, 50%, 75%, 100%, 130% of axial chord length respectively. It can be found that the rib structure significantly changes the outflow position of the leakage flow which is closer to the leading edge of the blade. Combined with the analysis of the third quarter, the arrangement of the first layer of ribs prevent a part of the mainstream from entering the cavity. As a result, the transverse movement of the leakage flow is weakened, and more leakage flow is suction out by the passage vortex, thereby, reducing the backflow range of the

leakage flow in the corner area. In consequence, the inhibitory effect of Case 1 on the secondary flow is more obvious, the range of the high loss zone is significantly reduced.

Table 3 shows the comparison about mass average of total pressure loss coefficients at S3 sections. The loss coefficient of Case 1 is greater than that of Case 2. The percentage reduction of the two sections at 130% are 3.49% and 2.14% respectively.

Table 3. *Total pressure loss of S3 section about different schemes.*

| Axial chord length	25%	50%	75%	100%	130%
Case0	0.2391	0.2465	0.2538	0.2807	0.2545
Case1	0.2318	0.2361	0.2449	0.2780	0.2454
Case2	0.2343	0.2384	0.2476	0.2804	0.2493
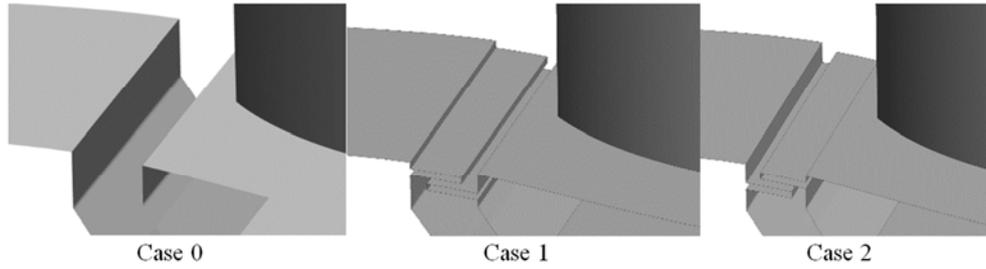
Figure 11. *Upstream cavity rib scheme.*
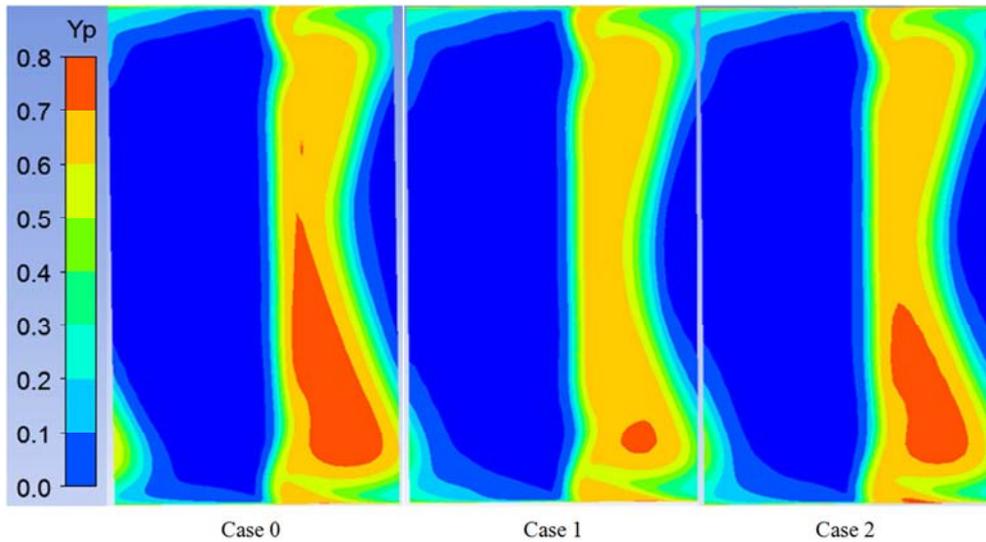
Figure 12. *Distribution of total pressure loss at 130% axial chord length.*


Case 0

Case 1

Case 2
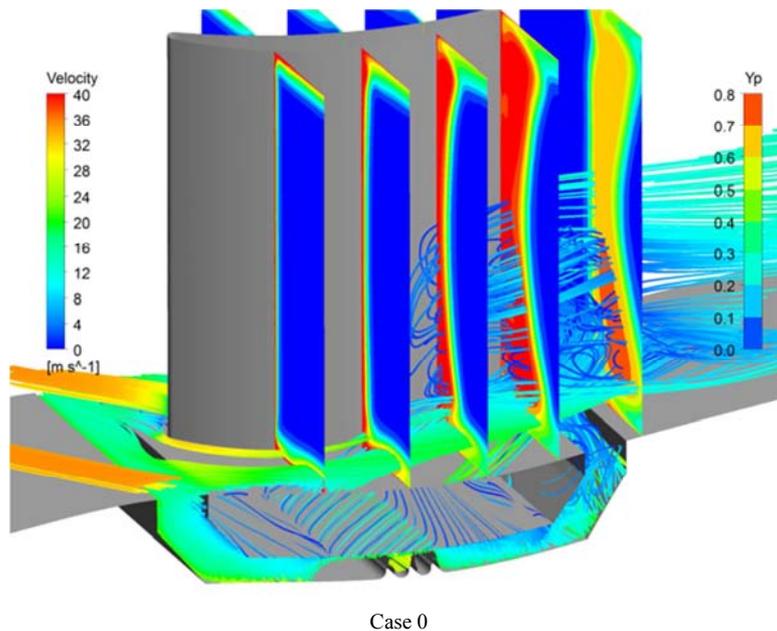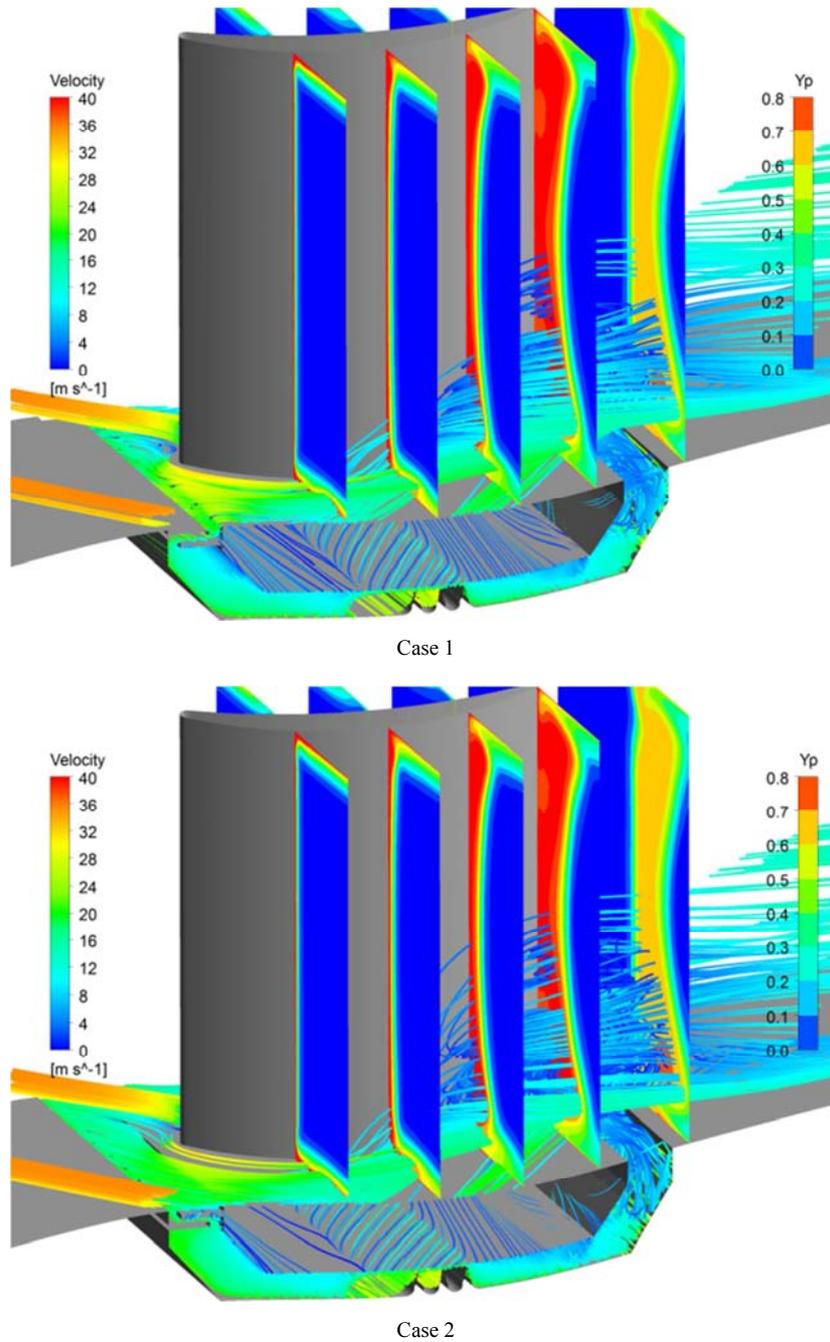
***Figure 13.** Distribution of total pressure loss and leakage flow of different case.*

5. Conclusions

This paper numerically calculates the static stator model of the compressor to analyze the secondary flow structure and leakage flow structure formed by the mainstream in the upstream cavity. Based on this, the upstream cavity configuration was optimized, and the following conclusions were drawn:

When the main stream flows through the upstream cavity, part of the fluid enters to upstream cavity at the leading edge of the blade, and then, blended with the leakage flow and eventually merged into the mainstream. This part of the flow is called the secondary flow of upstream cavity, which can affect 80% height range. The secondary flow of upstream cavity and leakage flow of the upstream cavity constitute a secondary flow at the root of the stator channel.

The influence of leakage flow in the flow direction is mostly reflected in the first half of the flow field and the wake area. When there is leakage, the degree of flow difference in the near casing area is almost constant, but the difference in flow between blade root and middle is greatly increased. Reducing the leakage gap decreases the flow rate of the leakage flow, at the same time, increasing the flow rate of the secondary flow and the loss caused by the secondary flow of the upstream cavity is not negligible.

The addition of rib structure on both side walls of the cavity can reduce the secondary flow of upstream cavity and reduce the total pressure loss of the S3 section of the channel. The flow structure of the cascade channel has obvious changes, and the flow performance is improved. In addition, the research shows that the first layer of ribs is better at the wall surface of the hub, and the percentage of total pressure loss coefficient decreases by about 3.49%.

Nomenclature

C	True chord (mm)
S	Blade pitch (mm)
τ	Cascade solidity
k_1	Inlet blade (material) angle (°)
h	Cavity depth (mm)
C_z	Axial chord (mm)
H	Blade span (mm)
ε	Seal-clearance (mm)
k_2	Exit blade (material) angle (°)
d	Cavity width (mm)

References

[1] Campobasso M. S, Mattheiss A, Wenger U, et al. Complementary use of CFD and experimental measurements to assess the impact of shrouded and cantilevered stators in axial compressors. *ASME International Gas Turbine and Aeroengine Congress and Exhibition*, Indianapolis, Indiana, USA, 1999.

[2] Yoon S, Selmeier R, Cargill P, et al. Effect of the stator hub configuration and stage design parameters on aerodynamic loss in axial compressors. *J Turbomach,* 2015, 137 (9): 091001.

[3] Zi-nan Wang. Experimental and numerical investigation on endwall flow of cantilevered stator in axial compressor. *The University of Chinese Academy of Sciences*. Beijing, China, 2016.

[4] Geoffrey J. Sturgess. Application of CFD to gas turbine engine secondary flow system-the labyrinth seal. In: *AIAA/ASME/SAE/ASEE 24th joint propulsion conference*, Boston, Massachusetts, 1988.

[5] Wellborn S. R. and Okiishi T. H. Effects of shrouded stator cavity flows on multistage axial compressor aerodynamic performance. Iowa State University: NASA, CR-198536, 1996; 90-101.

[6] Wellborn S. R., Okiishi T. H. The influence of shrouded stator cavity flows on multistage compressor performance. *J Turbomach* 1999; 121 (3), pp.486-497.

[7] Wellborn S. R., Tolchinsky I. Modeling shrouded stator cavity flows in axial flow compressors. *J Turbomach* 2000; 122 (1), 55-61.

[8] Heidegger N, Hall E, Delaney R. Parameterized study of high-speed compressor seal cavity flow [C]//Joint Propulsion Conference & Exhibit. 1996.

[9] Popovic I. and Hodson H. P. The effects of a parametric variation of the rim seal geometry on the interaction between hub leakage and mainstream flows in high pressure turbines. *J Eng Gas Turb Power* 2012; 135 (11), 1823-1833.

[10] Demargne A. and Longley J. P. The aerodynamic interaction of stator shroud leakage and mainstream flows in compressors. *ASME Turbo Expo Power for Land Sea and Air*, Munich, Germany, 2000; paper no.2000-GT-0570.

[11] Kim J. W., Song S. J. and Kim T. Streamwise evolution of loss in a shrouded axial compressor cascade passage. *AIAA J Propul Power*, 2011; 27 (4), 884-889.

[12] Sohn D. W., Kim T. and Song S. J. Influence of the leakage flow tangential velocity on the loss generation and leakage flow kinematics in shrouded axial compressor cascades. *51st ASME Turbo Expo,* Barcelona, Spain, 2006; 389-397.

[13] Xin. Fu., Wan-yue. Wang, and Yan. Zhang. Simulation of the flow structure of the mainstream in the upstream cavity in an axial compressor. *Ordnance Industry Automation*, 2018; 37 (07), 83-88.

[14] Yong-hua. Cao. A study based on using jet to suppress leakage flow in the labyrinth seal. *Nanjing University of Aeronautics and Astronautics*, 2017.

[15] Jian-feng. Zhu, Guo-ping. Huang, and Xin. Fu. Preliminary experiment of suppressing flow separation in cascade by micro pulsed jet without external device. *Journal of Aerospace Power*, 2014; 29 (02), 391-397.